Mem. S.A.It. Suppl. Vol. 1, 36

Memorie della
Supplementi

Riemann solver in SPH

D. Molteni[1], C. Bilello[2]

[1] Dipartimento di Fisica et Tecnologie Relative, Universitá degli Studi di Palermo, Viale delle Scienze, 90128 Palermo. e-mail: molteni@unipa.it

[2] Dipartimento di Ingegneria Strutturale e Geotecnica, Universitá degli Studi di Palermo, Viale delle Scienze, 90128 Palermo.e-mail: bilello@diseg.unipa.it

Abstract.
Two approaches are presented for the solution of shocks in fluid dynamic problems discretized through meshless methods. The proposed methods are based on the use of the analytical solution for the Riemann problem and belong to the class of Goudunov methods. The advantage of using such methods lies in the fact that no artificial viscosity is required. Moreover, from numerical tests on a classical 1D Sod'problem and a on 2D shock around a Black Hole, it has been observed that the accuracy of the solution is greatly improved.

Key words. Computational Fluid Dynamics – Lagrangean Methods – Shocks – Black Holes – GSPH

1. Introduction

One of the most accurate way to calculate shocks formation and their evolution, integrating the system of hyperbolic equations governing the fluid motion, is the Godunov approach (Godunov, 1959). Its accuracy, for the shock treatment, is due the idea of exploiting the analytical solution of the Riemann problem: it is possible to calculate analytically the time evolution of a true discontinuity of the variables defining the fluxes. This technique is widely used in many numerical schemes that are sophisticated evolutions of the basic Godunov idea (LeVeque 1992).
However, it is well known that for some problems like mixing of different fluid components a Lagrangian approach is desiderable. Lagrangian approach is traditionally known to be unpractical for large deformations of the flow, since the eventual grid deformation make impossible plain techniques of partial derivatives evaluation. However, in the last decade, a large interest is grown on the so called meshless methods. One of the first and very simple meshless method is know as Smoothed Particles Hydrodynamics (Monaghan, 1992). Recently the mathematical basis of these methods have been analyzed and greatly developed. In the engineering field these methods are known as MLSQI (Moving Least Square Interpolants) or

Send offprint requests to: D. Molteni
Correspondence to: Dipartimento di Fisica e Tecnologie Relative, Universitá degli Studi di Palermo, Viale delle Scienze, 90128 Palermo.

RKPM (Reproducing Kernel Particles Method). In these methods the derivatives are evaluated in a very accurate way even in a set of disordered nodes (Belytschko et al., 1996; Chen et al., 2000). However the shock treatment in these last methods is still essentially based on the use of artificial viscosity (A.V.) terms. This A.V. approach has many drawbacks and it seems desiderable the use of Godunov approach even in the SPH methods. Few studies appeared on this subject. Recently Parshikov (Parshikov et al. 2000) describes a Godunov-SPH method having good shock treatment capabilities. He solves the Riemann problem arising from the interaction between one particle and each of its neighbors, then he calculates the forces on the moving node as an average over the intermediate Riemann values, but it is only first order accurate and it seems very CPU time consuming, since it solves the Riemann problem between each node and its neighbor ones. Another approach has been very synthetically described by Inutsuka (Inutsuka, 1994). His results seem very accurate and his formulae are promising, but they lack a solid mathematical foundation and no details appeared in the literature.

Our work starts from the basic Inutsuka idea but it offers a better understanding of the proposed formulae. In Section 2 the fundamental equation governing the fluid dynamics problem for a perfect fluid are briefly introduced. In Section 3 we review the basic SPH interpolation ideas and describe the equations we use. In Section 4 and 5 we describe the implementation of Godunov approach in the SPH framework. In Section 6 we show the test cases compared with analytical solutions. The conclusions follow in the final section.

2. Governing Equations

The dynamic equations for an incompressible non-viscid fluid are written in a Lagrangean formulation as (Aris, 1990)

Continuity equation

$$\frac{D\rho}{Dt} = -\rho \nabla \cdot \mathbf{v} \tag{1}$$

Momentum equation

$$\frac{D\mathbf{v}}{Dt} = \mathbf{f} - \frac{1}{\rho}\nabla p \tag{2}$$

Energy equation

$$\frac{D\varepsilon}{Dt} = \frac{1}{\rho}\mathbf{T}{:}\nabla \cdot \mathbf{v} \tag{3}$$

State equation

$$p = (\gamma - 1)\,\rho\varepsilon \tag{4}$$

where ρ is the density, $\mathbf{v}$ is the velocity vector, $\mathbf{f}$ is the external or body force vector, p is the internal pressure, ε is the thermal energy per unit mass, $\mathbf{T}$ is the stress tensor, γ is the polytropic constant and D/Dt denotes comoving derivative.

In the most general case the stress tensor is given by

$$\mathbf{T} = -p\mathbf{I} + \mathbf{P}, \tag{5}$$

in which $\mathbf{P}$ denotes the viscous stress tensor. However, for a perfect fluid the stress is hydrostatic, i.e. $T_{ij} = -p\delta_{ij}$, and the equation of energy is rewritten in the form

$$\frac{D\varepsilon}{Dt} = -\frac{p}{\rho}\nabla \cdot \mathbf{v}. \tag{6}$$

The energy equation may also be written in terms of the specific total energy,

$$U = \varepsilon + \frac{1}{2}\mathbf{v}^2. \tag{7}$$

whose Lagrangean derivative may be calculated as

$$\frac{DU}{Dt} = -\frac{1}{\rho}\nabla \cdot (p\mathbf{v}) + \mathbf{f} \cdot \mathbf{v} \tag{8}$$

In conclusion, if the body forces are zero the fluid dynamic equation are

$$\frac{D\rho}{Dt} = -\rho \nabla \cdot \mathbf{v} \tag{9}$$

$$\frac{D\mathbf{v}}{Dt} = -\frac{1}{\rho}\nabla p \tag{10}$$

$$\frac{DU}{Dt} = -\frac{1}{\rho}\nabla \cdot (p\mathbf{v}) \tag{11}$$

whereas the state equation (4) still holds.

It is worth noticing that in eqs. (9-11) the space derivatives are evaluated at constant time level. The solution of the set of partial differential equations (9-11) is obtained through a spatial discretization.

In the next section the standard SPH expression for eq. (9-11) is reported.

3. The SPH formulation of the problem

There is a variety of forms Gingold and Monaghan, (1997) for the SPH formulation of the problem described in Section 2. As an example the following symmetric approximation of the hydrodynamic equation may be used

$$\frac{D\rho_i}{Dt} = -\rho_i \sum_k \frac{m_k}{\rho_k} (\mathbf{v}_i - \mathbf{v}_k) \cdot \nabla_i W_{ik} \tag{12}$$

$$\frac{D\mathbf{v}_i}{Dt} = -\sum_k m_k \left(\frac{p_i}{\rho_i^2} + \frac{p_k}{\rho_k^2} \right) \cdot \nabla_i W_{ik} \tag{13}$$

$$\frac{DU_i}{Dt} = -\frac{1}{\rho_i} \sum_k \frac{m_k}{\rho_k} [(p_i \mathbf{v}_i + -p_k \mathbf{v}_k)] \cdot \nabla_i W_{ik} \tag{14}$$

where $W_{ik} = W_{ik}(\mathbf{r}_i - \mathbf{r}_k, h_i, h_k)$ is the smoothing kernel, $\mathbf{r}_i = (r_{i1}, r_{i2}, r_{i3})$ is the position vector of the ith particle with respect to a cartesian reference system $\hat{\mathbf{x}}_1\hat{\mathbf{x}}_2\hat{\mathbf{x}}_3$and h_i is the smoothing distance.

The solution of Eq. (12) can be calculated in the form

$$\rho_i = \sum_k m_k W_{ik}. \tag{15}$$

Such expression is shown to satisfy the differential continuity equation since the conservation of mass is established from the very beginning.

The SPH method has been shown to be very effective for the solution of classical hydrodynamic problems. However for shock treatment an artificial viscosity (A. V.) must be taken into account to recover the numerical instability of the standard SPH solution. However, through the use of advanced numerical methods, it is possible to avoid the introduction of the A.V.

4. Godunov Method

Recently advantages have been obtained from the use of the Godunov approach combined with SPH (Inutsuka, 1994; Parshikov et al. 2000; Monaghan, 1997). This approach is based on the use of the analytical solution of the Riemann problem that provides the evolution of flow variables at a true one-dimensional discontinuity.

The Godunov method has been originally developed for one-dimensional hydrodynamic problems; moreover its original formulation is based on a cell discretization as shortly described herein.

Let's denote by p_i^{ah} and v_i^{ah} (scalar in a one-dimensional case) the pressure and velocity obtained by the solution of the Riemann problem associated, respectively, to particles ith and (i+1)th (ahead interface state), and by p_i^{be} and v_i^{be} those associated to particles (i-1)th and ith (behind interface state) (Fig. 1).

According to Godunov method the evolution of flow variables at the particle ith is calculated as

$$\rho_i^{n+1} = \rho_i^n - 2\rho_i^n \frac{v_i^{ah} - v_i^{be}}{\Delta x_i}\Delta t \tag{16}$$

$$v_i^{n+1} = v_i^n - 2\frac{p_i^{ah} - p_i^{be}}{\rho_i^n \Delta x_i}\Delta t \tag{17}$$

$$U_i^{n+1} = U_i^n - 2\frac{p_i^{ah} v_i^{ah} - p_i^{be} v_i^{be}}{\rho_i^n \Delta x_i}\Delta t. \tag{18}$$

in which the apex denotes the time step, $\Delta x_i = x_{i+1} - x_{i-1}$ and Δt has to be evaluated according to Courant criterion

$$\Delta t = \min\left(\frac{a\Delta x_i/2}{\sqrt{C_i^2 + v_i^2}} \right). \tag{19}$$

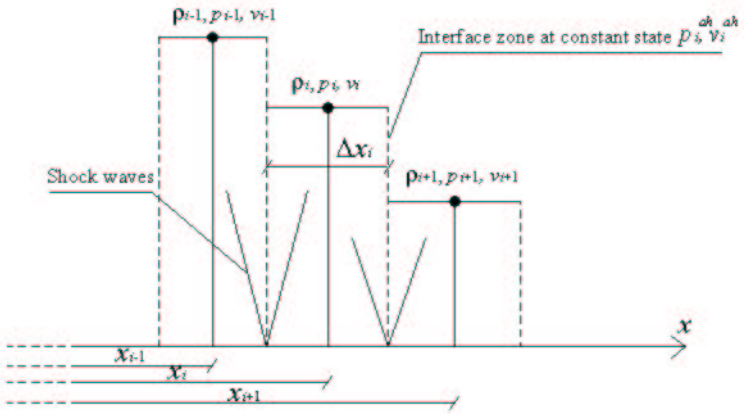

Fig. 1. Godunov scheme.

In Eq. (19) $a \leq 0.5$ and $C_i = \sqrt{\gamma\ p_i/\rho_i}$ is the sound speed at the position of particle ith.

It is apparent that for a SPH discretization of the hydrodynamic problem as well as for a two- or three-dimensional extension of this approach, one must perform an adequate interpolation of the flow variables of those particles lying in the support of the ith one (Inutsuka, 1994; Parshikov et al. 2000; Monaghan, 1997). These approaches are known as Godunov-SPH methods.

5. Proposed Godunov-SPH Methods

In this section two different Riemann solution-based methods, belonging to the class of Godunov SPH methods (GSPH), are presented.

In order to develop a generalized Godunov approach it is necessary to define the equivalent *ahead* and *behind* states. Moreover one has also to consider the dimension of the problem that introduces a question about which direction must be taken into account to define such states. This issue is discussed herein.

5.1. Method 1

Let's denote by ρ_k, p_k,$\mathbf{v}_k$ the actual flow state of those particles interacting with the ith one. The interaction condition is stated by the expression

$$|\mathbf{r}_k - \mathbf{r}_i| \leq 2h_{ik} = h_i + h_k. \tag{20}$$

For each interacting particle a one dimensional Riemann problem is solved along the direction $\mathbf{r}_k - \mathbf{r}_i$. The input states are given by ρ_i, p_i,v_i^{ik} and ρ_k, p_k,v_k^{ik} where

$$v_i^{ik} = \mathbf{v}_i \cdot \frac{\mathbf{r}_k - \mathbf{r}_i}{|\mathbf{r}_k - \mathbf{r}_i|}; \tag{21}$$

$$v_k^{ik} = \mathbf{v}_k \cdot \frac{\mathbf{r}_k - \mathbf{r}_i}{|\mathbf{r}_k - \mathbf{r}_i|}. \tag{22}$$

The solution of such problem is denoted by p_R^{ik} and v_R^{ik}.

The equivalent ahead and behind flow variables are obtained by projecting the Riemann solution along a cartesian system $\hat{\mathbf{x}}_1\hat{\mathbf{x}}_2\hat{\mathbf{x}}_3$ originating in $\mathbf{r}_i$,

$$\left\langle p_{iq}^{ah} \right\rangle = \frac{\sum\limits_k \frac{m_k}{\rho_k} p_R^{ik} W_{ik_q}^{ah}}{M_{0_i}^{ah}}; \tag{23}$$

$$\left\langle v_{iq}^{ah} \right\rangle = \frac{\sum\limits_k \frac{m_k}{\rho_k} v_R^{ik} \Delta\hat{\mathbf{r}}_{ik} \cdot \hat{\mathbf{x}}_q W_{ik_q}^{ah}}{M_{0_i}^{ah}} \tag{24}$$

for q = 1,2,3 and $M_{0_i}^{ah} = \sum\limits_k \frac{m_k}{\rho_k} W_{ik_q}^{ah}$, $\Delta\hat{\mathbf{r}}_{ik} = (\mathbf{r}_k - \mathbf{r}_i)/|\mathbf{r}_k - \mathbf{r}_i|$.

In a similar way the equivalent interface distance is defined as

$$\left\langle \Delta x_{iq}^{ah} \right\rangle = \frac{\sum\limits_k \frac{m_k}{\rho_k} \left| (\mathbf{r}_k - \mathbf{r}_i) \cdot \hat{\mathbf{x}}_q \right| W_{ik_q}^{ah}}{M_{0_i}^{ah}} \quad (25)$$

for q = 1,2,3.

In Eqs. (23,24) and (25) $W_{ik_q}^{ah}$ is the ahead projected kernel

$$W_{ik_q}^{ah} = \begin{cases} W_{ik} \cos \vartheta_{ik_q}, & \text{if } \cos \vartheta_{ik_q} > 0 \\ 0, & \text{otherwise.} \end{cases} \quad (26)$$

and ϑ_{ik_q} is the angle between the direction of $\mathbf{r}_k - \mathbf{r}_i$ and $\hat{\mathbf{x}}_q$.

The behind state is simply obtained by replacing in Eqs. (23,24) and (25) $W_{ik_q}^{be}$ for $W_{ik_q}^{ah}$ where

$$W_{ik_q}^{be} = \begin{cases} W_{ik} \left| \cos \vartheta_{ik_q} \right|, & \text{if } \cos \vartheta_{ik_q} < 0 \\ 0, & \text{otherwise.} \end{cases} \quad (27)$$

Then the following assumptions are made

$$\langle \nabla \cdot \mathbf{v} \rangle_i = 2 \sum_{s=1}^{3} \frac{\left\langle v_{is}^{ah} \right\rangle - \left\langle v_{is}^{be} \right\rangle}{\langle \Delta x_{is} \rangle} \quad (28)$$

$$\langle \nabla p_q \rangle_i = 2 \frac{\left\langle p_{iq}^{ah} \right\rangle - \left\langle p_{iq}^{be} \right\rangle}{\langle \Delta x_{iq} \rangle}; \text{for q = 1,2,3} \quad (29)$$

$$\langle \nabla \cdot (p\mathbf{v}) \rangle_i = 2 \sum_{s=1}^{3} \frac{\left\langle p_i^{ah} \right\rangle \left\langle v_{is}^{ah} \right\rangle}{\langle \Delta x_{is} \rangle} + - \frac{\left\langle p_i^{be} \right\rangle \left\langle v_{is}^{be} \right\rangle}{\langle \Delta x_{is} \rangle} \quad (30)$$

in which $\langle \Delta x_{is} \rangle = \left\langle \Delta x_{is}^{ah} \right\rangle + \left\langle \Delta x_{is}^{be} \right\rangle$.

Finally, similarly to Eqs. (16-18), the evolution of flow variables for the ith particle is calculated as

$$\rho_i^{n+1} = \rho_i^n - \rho_i^n \langle \nabla \cdot \mathbf{v} \rangle_i \Delta t \quad (31)$$

$$v_{iq}^{n+1} = v_{iq}^n - \frac{\langle \nabla p_q \rangle_i}{\rho_i^n} \Delta t; \text{for q = 1,2,3} \quad (32)$$

$$U_i^{n+1} = U_i^n - \frac{\langle \nabla \cdot (p\mathbf{v}) \rangle_i}{\rho_i^n} \Delta t, \quad (33)$$

and Δt is given by

$$\Delta t = \min_i \min_k \frac{a \left| \mathbf{r}_k - \mathbf{r}_i \right| / 2}{\sqrt{C_i^2 + \left(v_i^{ik} \right)^2}}. \quad (34)$$

.

It is worth noticing that the method just described is very time consuming since they require the solution of $N_p \lg N_p$ Riemann problems (N_p is the total number of particles). This computational issue may be overcome by using numerical approximations of the Riemann solution.

5.2. Method 2

In order to reduce the computational issue outlined in the previous Section the flow variables of the particles in the support of ith may be projected directly along three orthogonal directions opportunely selected.

These directions may be different from particle to particle. Proceeding in this way one defines for each projection axis the position of two imaginary particles, one ahead and the other behind the ith one, whose flow states are calculated through a proper interpolation of the surrounding particles' states.

To show this let's denote by $\mathbf{x}_{i1}^*$, $\mathbf{x}_{i2}^*$ and $\mathbf{x}_{i3}^*$ three orthogonal unit vectors defining the projection axis at the ith particle (Fig. 2). Using a similar notation as in Section 5.1, the following interpolated quantities can be defined

$$\left\langle \rho_{iq}^{ah} \right\rangle = \frac{\sum\limits_k \frac{m_k}{\rho_k} \rho_k W_{ik_q}^{ah}}{M_{0_i}^{ah}}; \quad (35)$$

$$\left\langle p_{iq}^{ah} \right\rangle = \frac{\sum\limits_k \frac{m_k}{\rho_k} p_k W_{ik_q}^{ah}}{M_{0_i}^{ah}}; \quad (36)$$

$$\left\langle v_{iq}^{ah} \right\rangle = \frac{\sum\limits_k \frac{m_k}{\rho_k} \mathbf{v}_k \cdot \mathbf{x}_{iq}^* W_{ik_q}^{ah}}{M_{0_i}^{ah}}; \quad (37)$$

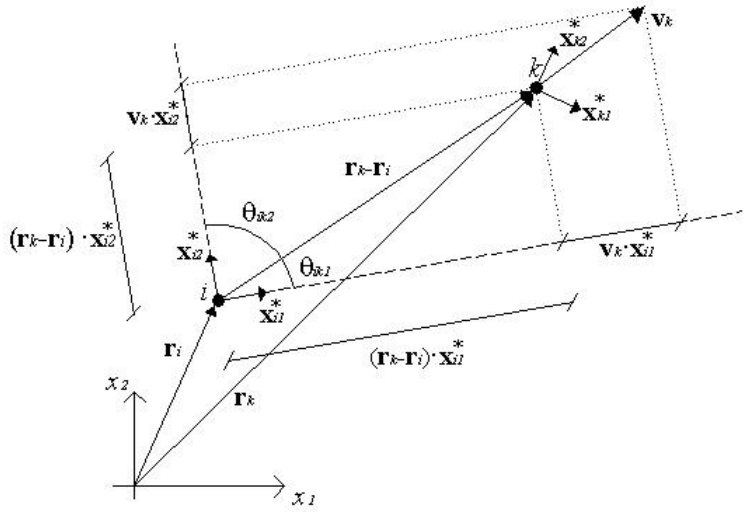

Fig. 2. Projection of the flow state along the direction $\mathbf{r}_k - \mathbf{r}_i$.

$$\left\langle \Delta x_{iq}^{ah} \right\rangle = \frac{\sum\limits_k \frac{m_k}{\rho_k} \left| (\mathbf{r}_k - \mathbf{r}_i) \cdot \mathbf{x}_{iq}^* \right| W_{ik_q}^{ah}}{M_{0_i}^{ah}} \quad (38)$$

for q = 1,2,3.

In Eq. (35-38) W_{ikq}^{ah} is still calculated from (26) where ϑ_{ikq} is now the angle between the direction of $\mathbf{r}_k - \mathbf{r}_i$ and $\mathbf{x}_{iq}^*$. In a similar way one can calculate the behind values.

Then for each particle and each projection axes two Riemann problems are solved: the first one using the input ρ_i, p_i,$\mathbf{v}_i \cdot \mathbf{x}_{iq}^*$ and $\left\langle \rho_{iq}^{ah} \right\rangle$, $\left\langle p_{iq}^{ah} \right\rangle$, $\left\langle v_{iq}^{ah} \right\rangle$, respectively, which provides the output $p_{iq}^{R\ ah}$ and $v_{iq}^{R\ ah}$, the second one using the input ρ_i, p_i,$\mathbf{v}_i \cdot \mathbf{x}_{iq}^*$ and $\left\langle \rho_{iq}^{be} \right\rangle$, $\left\langle p_{iq}^{be} \right\rangle$, $\left\langle v_{iq}^{be} \right\rangle$, respectively, which provides the output $p_{iq}^{R\ be}$ and $v_{iq}^{R\ be}$.

Using the solution of these Riemann problems the following interpolated spatial derivatives of the flow variables are defined

$$\left\langle \nabla \cdot \mathbf{v} \right\rangle_i = 2 \sum_{s=1}^{3} \frac{v_{is}^{R\ ah} - v_{is}^{R\ be}}{\left\langle \Delta x_{is} \right\rangle} \quad (39)$$

$$\left\langle \nabla p_q \right\rangle_i = 2 \sum_{s=1}^{3} \frac{\left(p_{is}^{R\ ah} - p_{is}^{R\ be} \right) \mathbf{x}_{is}^* \cdot \hat{\mathbf{x}}_q}{\left\langle \Delta x_{is} \right\rangle}; \quad \text{for q = 1,2,3} \quad (40)$$

$$\left\langle \nabla \cdot (p\mathbf{v}) \right\rangle_i = 2 \sum_{s=1}^{3} \frac{p_{is}^{R\ ah} v_{is}^{R\ ah}}{\left\langle \Delta x_{is} \right\rangle} + - \frac{p_{is}^{R\ be} v_{is}^{R\ be}}{\left\langle \Delta x_{is} \right\rangle} \quad (41)$$

where $\left\langle \Delta x_{is} \right\rangle = \left\langle \Delta x_{is}^{ah} \right\rangle + \left\langle \Delta x_{is}^{be} \right\rangle$.

The evolution of flow variables is finally obtained by substituting Eqs. (39-41) in (31-33). As for the time step Δt it must be so that

$$\Delta t = \min_i \ \min_q \frac{a \left\langle \Delta x_{iq} \right\rangle / 2}{\sqrt{C_i^2 + \left| \mathbf{v}_i \cdot \mathbf{x}_{iq}^* \right|^2}}. \quad (42)$$

It is worth noticing that, proceeding in this way, the original problem has been reduced to the solution of three one-dimensional problems.

The selection of the projection axes is totally arbitrary however in the numerical applications two cases have been investigated: in the first one they coincide with a cartesian reference system while in the second one they coincide with the principle axes of deformation.

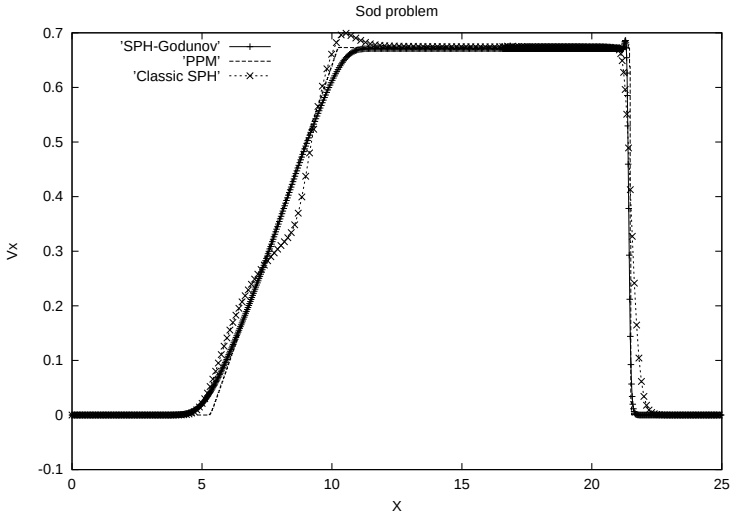

Fig. 3. Velocity profiles.

The latter case requires at each time step and for each particle the evaluation of the eigenvalues and eigenvectors of the deformation tensor.

6. Numerical Tests

Some numerical tests have been performed to validate the proposed solution methods. First the classical 1D shock tube problem (Sod, 1978) has been studied.

The following input values are selected: $\varrho_{Left} = 1.$, $p_{Left} = 1.$, $\varrho_{Right} = 0.25$, $p_{Right} = 0.175$. In Fig. 3 the velocity profile at time $t = 6.081$ is shown for the standard SPH code (with A.V. included), an high resolution PPM code and for the proposed GSPH code (Method 2).

In Fig. 4 a zoom of the shock front is reported. It is clear that GSPH solution is capable of reproducing the discontinuity in a better way. It is also worth noticing that the expansion fan is much better reproduced.

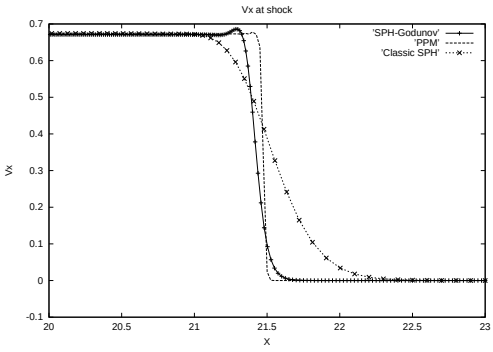

Fig. 4. Velocity profiles at shock front.

We also tested the code with a 2D problem of a shock formation around a black hole. For this case it is also possible to find the analytical solution (see Molteni et al. (1999) for details). This study is very critical since the flow has relevant shear motion and therefore the shear numerical viscosity

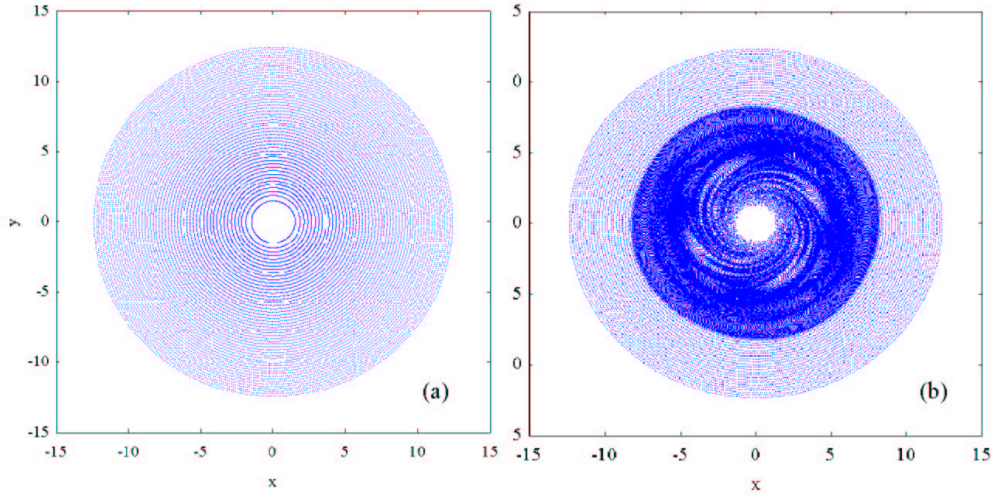

Fig. 5. Particle distribution: pre-shock (a) and post-shock (b)

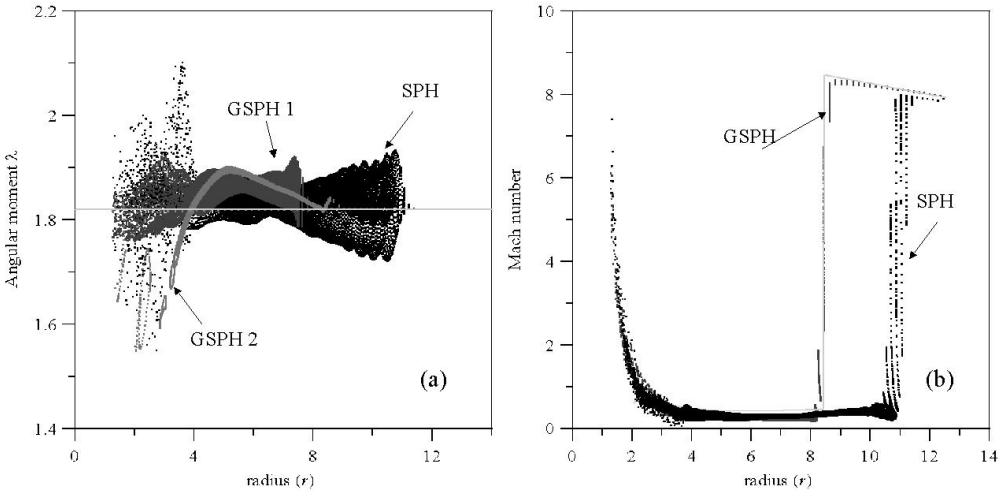

Fig. 6. Angular momentum(a) and radial Mach number (b) versus radial distance at the post-shock.

may strongly affect the results. In Fig. 5 the spatial distribution of the particles is shown in the pre-shock (Fig. 5a) and post-shock as well (Fig. 5b). The shock region is clearly characterized by an increase of the particles' density. Finally in Fig. 6 the angular momentum (Fig. 6a) and the radial Mach number (Fig. 6b) are reported versus the radial distance at a post-shock phase. Again, the analytical shock wave is better reproduced by the GSPH methods; however, due to large variations of the angular momentum (see Fig. 6a)has been observed that the shock position is not stable in time.

7. Conclusions

We reformulated SPH code adopting Riemann solvers to avoid the use of the classical artificial viscosity. We tested the code comparing its results with the analytical solutions of the 1D Sod tube problem and 2D circular shock around a Black Hole. With this new method the shock is much better resolved even in its first order formulation as presented in this work. We are developing higher order Riemann solution methods based on more refined interpolation criteria as MLSI and RKPM.

References

Aris, R. 1962, Prentice-Hall,Englewood Cliffs, N.J.

Belitschko, T., Krongauz, Y., R. A. , Organ, D. Fleming M. and Krysl,P. 1996, Comp. Methods Appl. Mech. Engrg., 139, pp. 3-47

Chen, J. K. and Beraun, J. E. 2000, Comp. Methods Appl. Mech. Engrg., 190, pp. 225-239

LeVeque, R. J. 1992, Basel: Birkhäuser Verlag.

Gingold, R. A. and Monaghan, J. J. 1977, MNRAS 181,375

Godunov, S. K. 1959, Mat. Sb., 47, 271

Inutsuka S. 1994, Mem. Soc. Astron. It, 65, pp. 1027

Molteni, D., Tth G., Kuznetsov, O. A. 1999, ApJ 516, pp. 411-419

Monaghan J. J. 1992, Annu. Rev. Astrom. Astrophys., 30, pp. 543-574

Monaghan J. J. 1997, J. Comp. Physics, 136, pp. 298-307

Parshikov, A. N., Medin, S. A., Loukashenko, I. I. And Milekin, V. A. 2000, Int. J. of Impact Engr., 24, pp. 779-796

Sod, G. , 1978, J. Comput. Phys., pp. 1-31